Steel and Composite Structures, *Vol. 26, No. 6 (2018) 759-769*
DOI: https://doi.org/10.12989/scs.2018.26.6.759

Shear and tensile behaviors of headed stud connectors in double skin composite shear wall

Jia-Bao Yan [1a], Zhe Wang [1b], Tao Wang [*2] and Xiao-Ting Wang [2,3c]

[1] *School of Civil Engineering / Key Laboratory of Coast Civil Structure Safety of Ministry of Education, Tianjin University, Tianjin 300350, China*
[2] *Key Laboratory of Earthquake Engineering and Engineering Vibration, Institute of Engineering Mechanics, CEA, Harbin 150080, China*
[3] *Department of Civil Engineering, Tsinghua University, Beijing 100084, China*

(*Received November 29, 2017, Revised January 1, 2018, Accepted January 20, 2018*)

Abstract. This paper studies shear and tensile behaviors of headed stud connectors in double skin composite (DSC) structure. Firstly, 11 push-out tests and 11 tensile tests were performed to investigate the ultimate shear and tensile behaviors of headed stud in DSC shear wall, respectively. The main parameters investigated in this test program were height and layout of headed stud connectors. The test results reported the representative failure modes of headed studs in DSC structures subjected to shear and tension. The shear-slip and tension-elongation behaviors of headed studs in DSC structures were also reported. Influences of different parameters on these shear-slip and tension-elongation behaviors of headed studs were discussed and analyzed. Analytical models were also developed to predict the ultimate shear and tensile resistances of headed stud connectors in DSC shear walls. The developed analytical model incorporated the influence of the dense layout of headed studs in DSC shear walls. The validations of analytical predictions against 22 test results confirmed the accuracy of developed analytical models.

Keywords: headed stud; shear resistance; tensile resistance; sandwich shear wall; double skin composite shear wall; steel-concrete composite shear wall

1. Introduction

Double skin composite (DSC) structure is a relative new type of structure that was originally developed for an immersed tube tunnel in UK (Tomlinson *et al*. 1990, Nie *et al*. 2013). Since then, this type of structure develops fast and exhibits versatile applications as shear wall, bridge deck, nuclear construction walls, oil containers, offshore decking, protective structures, shield tunnels, and ice-resistant wall in the Arctic offshore structures (Yan *et al*. 2016). More recently, research interests have been attracted to DSC shear walls used in high-rise buildings (Nie *et al*. 2013, Ji *et al*. 2015, 2017) and nuclear facilities (Kurt *et al*. 2016, Sener and Varma 2014, Zhang *et al*. 2014). A typical DSC composite structure usually comprises three layers of materials, i.e., a concrete core and two external layers of steel face plates. Different mechanical shear connectors or chemical bonding measures were used to bond the concrete core and two external steel faceplates together and make sure them working compositely. Friction-welded straight bar connectors have been developed for 'Bi-steel' type of DSC structure by Xie and Chapman (2005). However, the equipment for the friction-welding limited the depth of DSC structures within 0.2~0.7 m. Angle connectors were widely adopted for DSC structures in Japan (Malek *et al*. 1993). Due to the shallow anchoring depth, peeling off failure of the angle connectors compromised the integrity of DSC structures. Laser-welded corrugated steel strip connectors have been used in DSC structures by Leekitwattana *et al*. (2011). However, the laser-welding technology limits the thickness of the steel face plates used in the DSC structure. Headed stud connectors may be the most widely used shear connectors in steel-concrete and DSC composite structures (Shanmugam *et al*. 2002, Wright *et al*. 1991). Wright *et al*. (1991), Roberts and Dogan (1998), and Narayanan *et al*. (1997) developed the 'Double skin' composite structure using overlapped headed shear studs. This type of structure exhibits versatile advantages in terms of easy construction, saving site labor force and formworks, increased construction efficiency and shortened construction period, and high resistances under different loading scenarios (Nie *et al*. 2013, Hu *et al*. 2014, Yan *et al*. 2015). Thus, this paper develops the DSC shear walls with overlapped headed shear studs as shown in Fig. 1.

Headed stud connectors play essential roles in a DSC shear wall. As shown in Fig. 1, since the DSC shear walls were under applied axial compression and bending moment, headed studs firstly provide interfacial shear resistance along the steel-concrete interface that guarantee the composite action of a cross section; secondly, under compression, the steel face plates in the DSC composite wall tend to buckle outwards and would be pulled back by the headed studs welded to them, and the headed studs were thus under tension and their tensile resistances significantly influences the compressive resistance of steel surface plates.

*Corresponding author, Professor,
E-mail: wangtao@iem.ac.cn
[a] Associate Professor, E-mail: ceeyanj@163.com
[b] Master Student, E-mail: hwzgml@163.com
[c] Research Fellow, E-mail: aphael0323@126.com

http://www.techno-press.org/?journal=scs&subpage=6
ISSN: 1229-9367 (Print), 1598-6233 (Online)

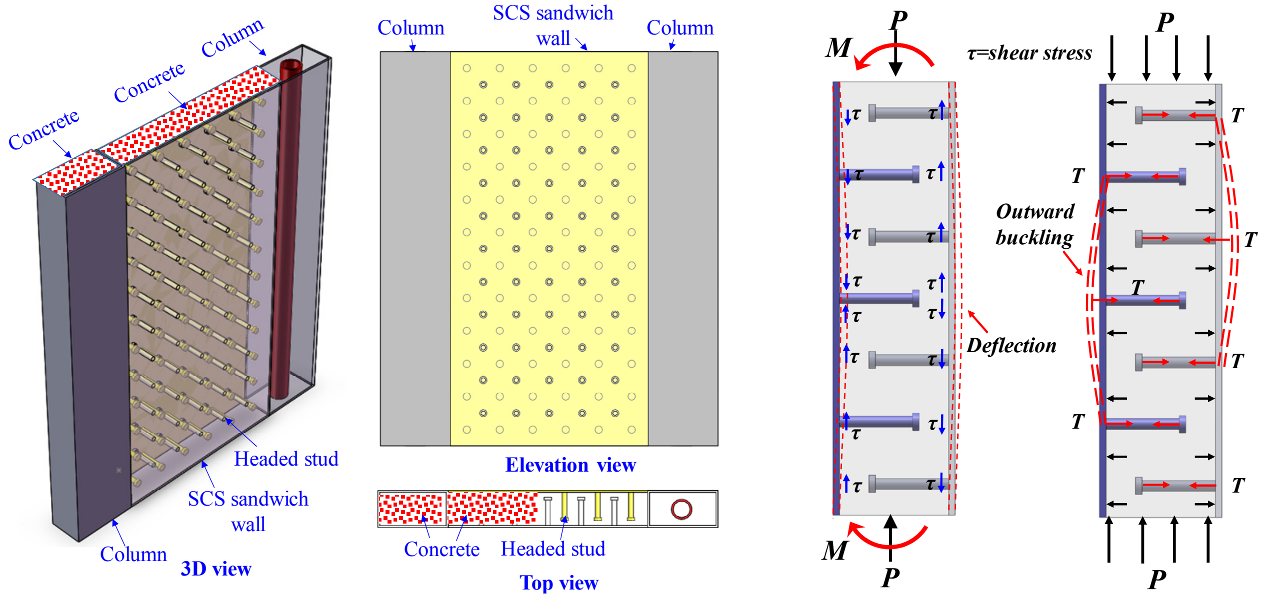

Fig. 1 DSC shear wall and internal stresses of headed studs

Thus, the shear and tensile resistances of headed studs are essential to the structural behaviors of DSC shear wall structures.

The shear resistance of headed studs is usually obtained through standard push-out tests as specified in different design codes, e.g., Eurocode 4 (2004). Extensive experimental studies have been reported on the shear resistance of headed studs through standard push-out tests. Viest (1957) performed the pilot push-out tests on headed studs in steel-concrete composite structures. Ollgaard *et al*. (1971) investigate the shear resistance of headed studs in steel-concrete composite structures with normal and lightweight concrete. Based on their push-out test results, the design equations were developed and incorporated in the design codes of many countries, e.g, Eurocode 4 (2004), ANSI/AISC (2010), and AASHTO (2004). Continuous push-out tests were performed by Oehlers and Johnson (1987), An and Cederwall (1996), Slobodan and Dragoljub (2002), Xue *et al*. (2008), and Han *et al*. (2015, 2017). These works promote the applications of steel-concrete composite beams or slabs in the buildings or bridges. However, the specimens for all these push-out tests typically consist of an I-beam with welded headed studs and two concrete slabs that simulates the working state of headed studs in steel-concrete composite structures. This tends to be different from the working state of headed studs in the DSC shear wall structure where the headed studs were mainly welded to two external steel face plates. Thus, it is of interest to carry out the push-out tests that could properly simulate the working state of the headed studs in DSC shear walls.

Tensile resistance of the single headed stud in concrete has also been studied through direct tensile tests. The tensile tests on the headed studs have been extensively reported by Fuchs *et al*. (1995), Lynch and Burdette (1991), Cook *et al.* (1992), Eligehausen and Balogh (1995), Zamora *et al.* (2003), and Hamad *et al*. (2011). As observed in these tensile tests, typical failure modes of a single headed stud under tension are tensile fracture of the steel shank, breakout out failure of the concrete slab, and pullout failure. Corresponding design equations on tensile resistance of the headed stud were provided in ACI 318 (2008) and ACI 349 (2001). However, these studies only focused on the tensile resistance of the headed studs that were used as the anchorage/fasteners in the reinforced concrete or prestressed concrete structures. The tensile tests were designed for the working state of the headed stud as anchorage/fasteners that were directly subjected to the tensile forces. This was different from headed studs in the DSC shear wall. It is necessary to propose a proper testing method that could appropriately reflect the working scenario of headed studs under tension in DSC structures. In addition, the information of experimental studies on tensile and shear resistances of headed studs in the DSC structure are still quite limited.

This paper experimentally studied the shear and tensile resistances of headed stud connectors in DSC shear wall structure. 11 push-out and 11 tensile tests were carried out to investigate the shear and tensile resistance of headed studs in DSC structure with normal weight concrete, respectively. Including the experimental studies, analytical models were also developed to evaluate the shear and tensile resistances of headed stud connectors used in DSC structures. Finally, corresponding design approaches were also proposed for the determinations of tensile and shear resistances of headed studs in DSC shear wall structure.

2. Test program

2.1 Push-out test on headed stud connectors in DSC structure

2.1.1 Specimens

In order to properly simulate the working state of headed shear studs in DSC structures, the push-out test

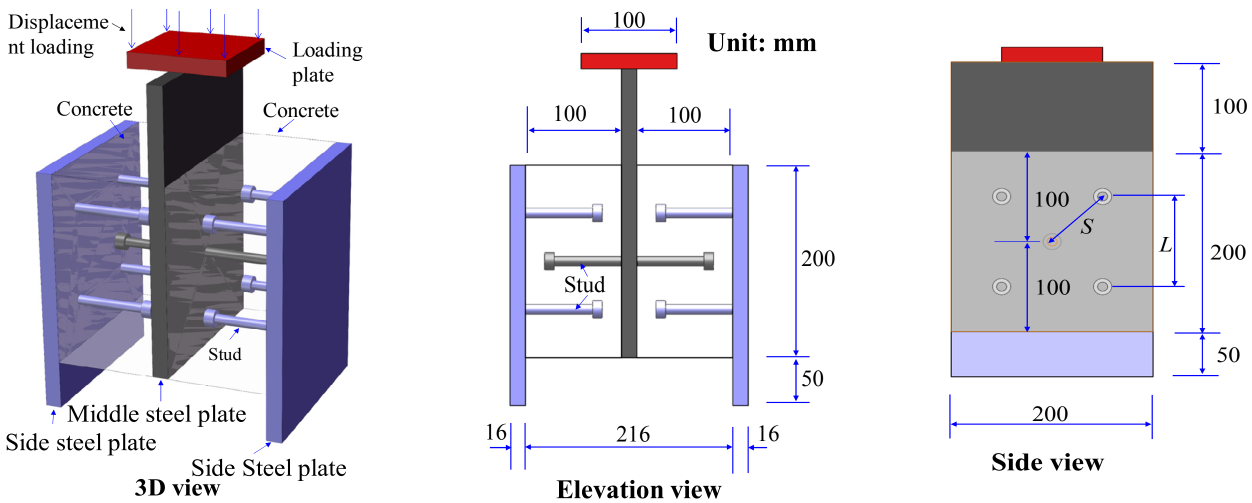

Fig. 2 Push-out test setup and details of specimens

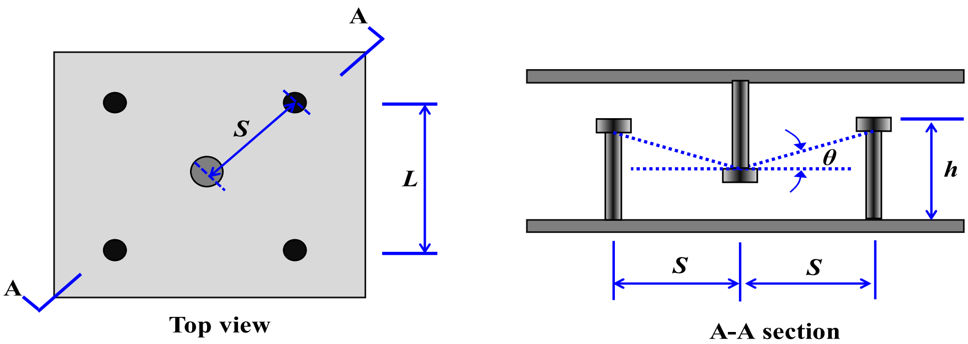

Fig. 3 Illustration on the geometric parameters in the push-out and tensile tests

specimen simulates a segment of the DSC shear wall as shown in Fig. 2. Different from the standard push-out test specimens in Eurocode 4 (2004), the push-out test specimen in this study used the steel plate instead of the I-beam as specified in Eurocode 4 (2004). As shown in Fig. 2, in order to offer close simulation on the working state of the headed stud connectors in the DSC shear wall, a typical push-out specimen is geometrically symmetric that consists of a middle steel plate with a pair of head studs welded on its two opposite surfaces, two concrete slabs, two side steel plates with four headed studs on each plate, and a loading plate. The four headed studs welded to the side steel plates provide the neighboring confinement on the headed stud welded to the middle steel plate. In order to avoid local buckling of the steel face plate under compression, 16 mm thick steel face plates were used. The diameter for the studs used in the push-out tests is 10 mm with varying heights for different specimens.

The thickness of the concrete slab equals to the typical thickness of a DSC shear wall of 100 mm. Fig. 3 shows the geometric details of connectors in the specimen for the push-out and tensile tests. It can be seen that with the given thickness of the DSC shear wall there are four parameters that can be used to describe the geometry of the specimen, i.e., spacing of the connectors in the side plates (L), spacing between the stud on the middle steel plate and side steel plate (S), height of the headed stud h, and the inclination angle (θ) between the lines connecting the heads of the stud connectors and the plane of the sandwich wall. Since with the given (h) and any two values of L, S, and (θ), the geometry of the specimen can be determined. Thus, before designing the test program for push-out test and tensile test, the two key parameters selected for the specimens are h and θ. Table 1 lists the details of the 11 push-out test specimens. The identical parameters are also selected for the 11 tensile test specimens even though there are different in geometries.

The headed studs with different heights of 60 mm, 70 mm, 80 mm, and 90 mm were studied in this test program. Thus, the 11 specimens can be categorized into four groups. In each group, different values of θ were used. More details of the push-out test specimens are listed in Table 1.

2.1.2 Materials in push-out test specimens

Grade C30 normal weight concrete with cubic compressive strength of 30.5 MPa was used in all the specimens. Q235 mild steel was adopted for the steel face plates. The elastic Young's modulus, yield and ultimate strengths for the 14 mm (or 16 mm) thick steel plate are 202 GPa (or 201 GPa), 278 MPa (or 290 MPa) and 417 MPa (or 472 MPa), respectively. The elastic Young's modulus, yield and ultimate strengths of the Φ10mm headed stud are 203 GPa, 420 MPa and 506 MPa, respectively.

Table 1 Details and results of push-out tests on headed stud in DSC shear wall

Item	h (mm)	θ (°)	S (mm)	L (mm)	Failure mode	P_T (kN)	P_E (kN)	P_T/P_E	P_A (kN)	P_T/P_A
S1	60	30	35	49	SP	32.9	29.3	1.12	33.7	0.97
S2	60	45	20	28	SP	39.6	29.3	1.35	33.7	1.17
S3	70	30	69	98	SP	32.0	29.3	1.09	33.7	0.95
S4	70	45	40	57	SP	38.8	29.3	1.32	33.7	1.15
S5	70	60	23	33	SP	32.5	29.3	1.11	33.7	0.96
S6	80	30	104	147	SP,WF	31.9	29.3	1.09	33.7	0.94
S7	80	45	60	85	SP	39.7	29.3	1.35	33.7	1.18
S8	80	60	35	49	SP,WF	46.7	29.3	1.59	33.7	1.38
S9	90	30	139	196	SP,WF	36.7	29.3	1.25	33.7	1.09
S10	90	45	80	113	SP,SS	43.7	29.3	1.49	33.7	1.30
S11	90	60	46	65	SP	31.6	29.3	1.08	33.7	0.94
Mean								1.26		1.09
Cov								0.14		0.14

*The diameter of headed stud in specimens S1~S10 is 10 mm; f_c and E_c for the concrete are 30.5 MPa and 33.0 GPa, respectively; f_y and f_u for the headed stud are 420 and 506 MPa, respectively; h denotes height of the headed stud; θ, S, and L are as shown in Fig. 3; P_T denotes experimental shear resistance of single headed stud; P_E denotes predicted shear resistance of single headed stud by Eurocode 4, i.e., Eq. (1); P_A denotes predicted shear resistance of single headed stud by AASHTO/LRFD (i.e. Eq. (3)); SP denotes splitting failure of the concrete core; WF denotes welding failure of the connector

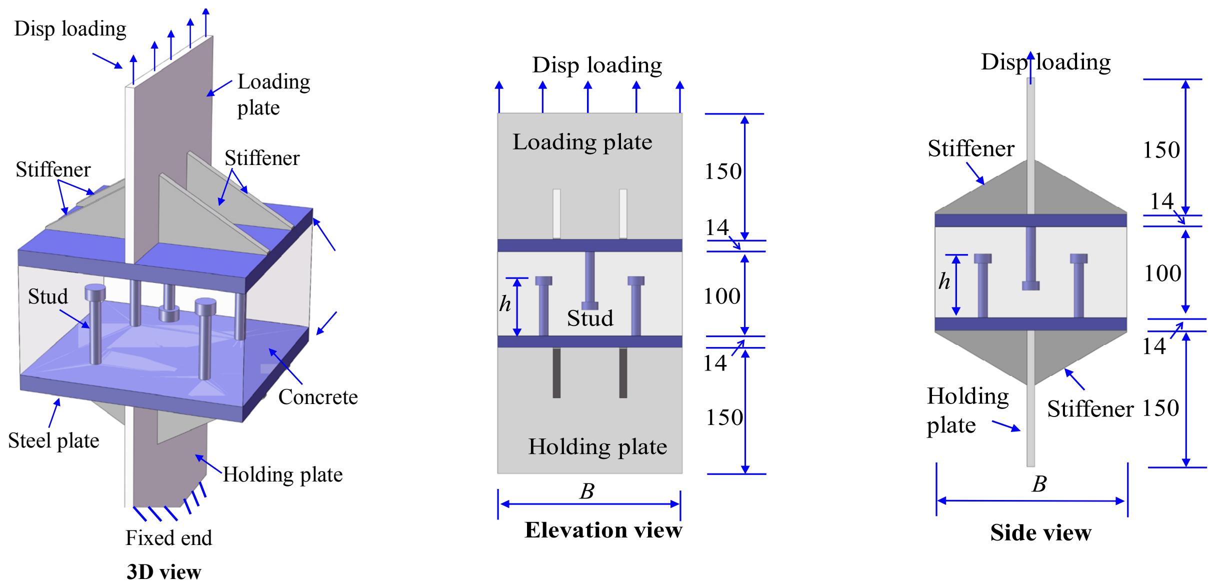

Fig. 4 Tensile test setup and details of specimens

2.1.3 Test setup and measurements

Fig. 2 shows test setup for the push-out tests on the headed stud in DSC shear walls. The specimen was firstly put on the rigid support, and displacement controlled type of loading with a rate of 0.1 mm/min was applied to the specimen through loading plate as shown in Fig. 2. Two linear varying displacement transducers (LVDTs) were installed under the loading plate and at the bottom end of the middle steel plate to record the interfacial slip between the concrete slab and middle steel plate. The reaction forces corresponding to different displacement levels were also recorded by a load cell adjunct to the actuator. All these readings including the displacement and reaction forces were recorded by the data logger connected an integrated system running on a PC.

2.2 Tensile tests on headed stud connectors in DSC structure

2.2.1 Tensile test specimens and material properties

Eleven specimens with identical parameters to the push-out test specimens were prepared for the tensile tests on headed stud connectors. Fig. 4 shows the representative specimen for the tensile tests on the headed studs in the DSC shear wall. Each specimen cuts a segment of the DSC shear wall with one headed stud on the top steel plate and four headed studs on the bottom steel plate. A loading plate and a holding plate were welded to the top and bottom steel plate, respectively. Stiffeners were also used to the connect the steel face plate to the loading or holding plate as shown in Fig. 3. The thickness of the steel face plate and concrete core are 14 mm and 100 mm, respectively. Similar to the push-out tests, the key parameters studied in the tensile tests are the height of the headed stud h, and the inclination angle θ between the lines connecting the heads of the stud connectors and the plane of the sandwich wall. Table 2 lists more details of the specimens in the tensile tests.

The same materials were used in the tensile tests as those in the push-out test specimens that can be found in Section 2.1.2.

2.2.2 Test setup and measurements

Fig. 4 shows the typical setup of the tensile tests. The holding plate was fixed to the bottom of the loading machines whilst the displacement type of loading with a rate of 0.1 mm/min was applied to the top loading plate. Two LVDTs were also installed on the top surface of the steel plate to record the elongation of the headed studs. The reaction forces relating to different elongation levels were also recorded by a data logger. All these readings that include the elongation, reaction force, and displacement loading were recorded by the data logger and controlled by an integrated system ruing on a PC.

3. Results of push-out tests on headed stud in DSC shear wall

3.1 General behavior and Failure modes

Figs. 5(a)~(d) shows the shear force, P, versus steel-concrete interfacial slip, Δ, relationships. This figure shows that all the P-Δ curves exhibit brittle recession behavior

Table 2 Details and results of tensile tests on headed stud in DSC shear wall

Item	h (mm)	θ (°)	S (mm)	L (mm)	Failure mode	T_T (kN)	T_A (kN)	T_T/T_A
T1	60	30	35	49	SP,BO,PO	32.8	23.2	1.41
T2	60	45	20	28	SP,PO	31.9	23.2	1.37
T3	70	30	69	98	SP,PO	33.6	31.2	1.08
T4	70	45	40	57	SP,PO	36.0	31.2	1.16
T5	70	60	23	33	SP,TF	38.6	31.2	1.24
T6	80	30	104	147	SP,BO	29.1	40.3	0.72
T7	80	45	60	85	SP,TF	36.9	40.3	0.92
T8	80	60	35	49	SP,TF	38.6	40.3	0.96
T9	90	30	139	196	SP,PO	43.6	42.9	1.01
T10	90	45	80	113	SP,PO	44.2	42.9	1.03
T11	90	60	46	65	SP,PO	39.3	42.9	0.92
Mean								1.07
Cov								0.19

*The diameter of headed stud in specimens T1~T10 is 10 mm; f_c and E_c for the concrete are 30.5 MPa and 33.0 GPa, respectively; f_y and f_u for the headed stud are 420 and 506 MPa, respectively; h denotes height of the headed stud; θ, S, and L are as shown in Fig. 3; T_T denotes experimental tensile resistance of the specimen; T_A denotes predicted tensile resistances of single connector by Eq. (4); BO, SP, PO, and TF denotes breakout, splitting, pullout, and tensile fracture failure mode, respectively

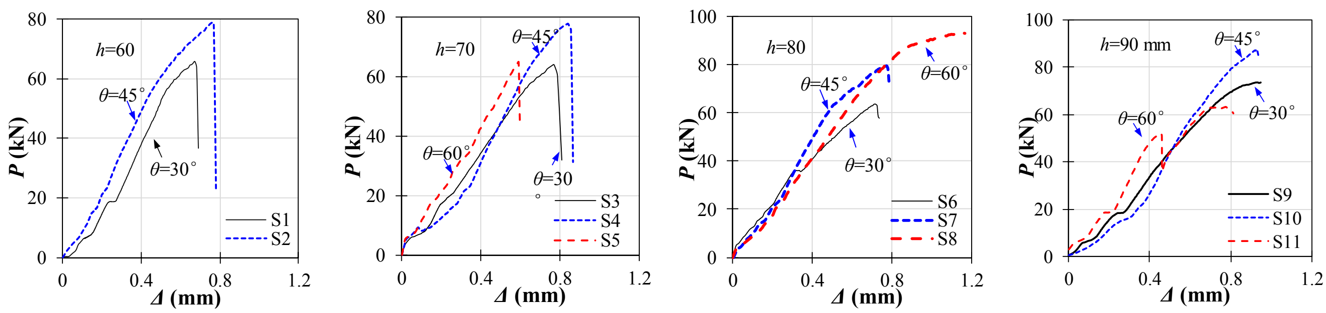

(a) Specimens S1~S2 (b) Specimens S3~S5 (c) Specimens S6~S8 (b) Specimens S9~S11

Fig. 5 Shear force versus slip behaviours of the push-out tests after the peak load that implies the brittle failure of the tested specimens. As the interfacial slip increases the reaction shear force firstly increases almost linearly to about 70%~80% of its ultimate resistance. Then, the headed stud started to yield that can be supported by evidence of the strain-slip curve as shown in Fig. 6. After that, the all the *P*-Δ curves of all the tested specimens exhibited very short nonlinear behaviors until achieving the ultimate resistances. After peak resistance, all the specimens exhibited brittle failure behavior that accompanied by concrete breakout or splitting. The brittle behaviors of the head studs in DSC shear walls were mainly due to the splitting or breakout failure of concrete that interrupted the fully development of the yielding plateau of the studs. Reinforcement mesh may be considered that enhanced the splitting resistance of the concrete core and deterred the splitting or breakout of the concrete core. Another reason of the low slip capacity of the headed studs in the push-out tests may be due to the low strength concrete used.

There were two types of failure mode observed from the tests, i.e., splitting failure of the concrete block and welding failure of the connectors. Fig. 7 shows these two types of failure mode. As shown in Figs. 7(a) and (b), the splitting failure mode is characterized by: (1) brittle behavior in the shear-slip curves; (2) the strain in the shank of the steel stud is much smaller than the fracture strain of the steel (see Fig. 6).

3.2 Effect of inclination angle θ

Fig. 8(a) shows the influence of the inclination angle (θ) on ultimate shear resistance of the push-out specimens (P_u). It can be found that as the value of θ increases from 30 degree to 45 degree the ultimate resistance averagely increases by about 20% for all the headed studs with different heights. This is because θ will increase the confinement of the concrete and delay the splitting failure of the concrete slab that finally resulted in larger shear

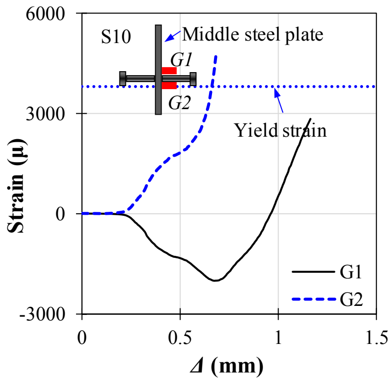

Fig. 6 Strain versus slip curves of specimen S10

(a) Splitting failure

(b) Welding failure of the connector

Fig. 7 Failure mode of the push-out test

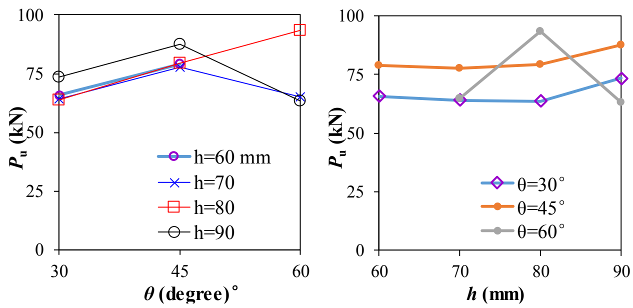

(a) Splitting failure
(b) Welding failure of the connector

Fig. 8 Effect of θ and h on ultiamte shear resistance of headed stud

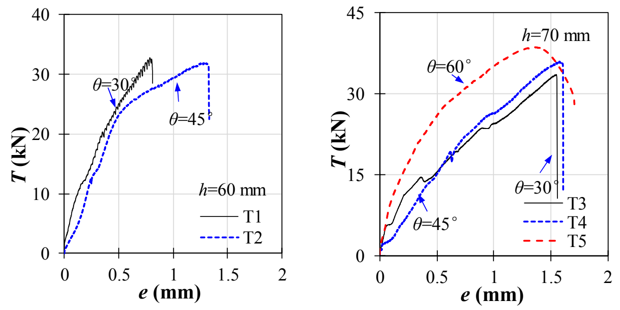

(a) Specimens T1~T2
(b) Specimens T3~T5

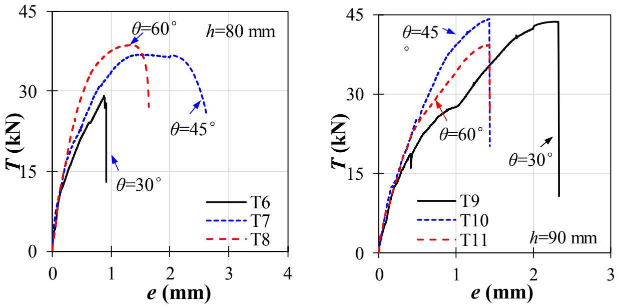

(c) Specimens T6~T8
(b) Specimens T9~T11

Fig. 9 Shear force versus slip behaviours of the push-out tests resistance of the headed studs. However, as the value of θ increases from 45 degree to 60 degree increasing θ did not has positive influence on the ultimate shear resistance of the headed studs.

3.3 Effect of height of the headed stud h

Fig. 8(b) shows the influence of the height of the headed stud h on the ultimate resistance of the headed stud. It can be observed that as the height of the headed stud increases from 60 mm to 90 mm, the shear resistance of the headed stud was slightly increased. This may be explained by that the specimens all failed in splitting mode and the splitting resistance of the specimen is more influenced by the tensile strength and size of the concrete slab. The height of the headed stud would thus have limited influence on the shear resistance for the headed stud failed in splitting mode.

4. Results of tensile tests on headed stud in DSC shear wall

4.1 General behavior and failure mode

Fig. 9 shows the tensile force versus elongation curves of the headed stud under tension. This figure shows that all the tensile force (T) versus elongation (e) curves exhibited three stages. At the first stage, the reaction tensile force T increases almost linearly with the increase of the elongation e. Gradually, at stage II, nonlinear behavior starts to develop due to yielding of the headed stud. At the third stage, the T-e curves of all the specimens show sudden drops that implies brittle failure mode of the headed stud.

There were four types of failure modes that were observed from the tensile tests, i.e., pullout failure, breakout failure of the concrete core, splitting failure of the concrte core, and tensile fracture failure of the headed stud. Pullout failure means the headed stud was pulled out from the concrete core due to the compression failure occurred to the concrete surrounding the head of the stud. The concrete breakout failure is characterized by that concrete cone is pulled out from the concrete block as shown in Fig. 10(a). Specimen T1 and T6 failed in this type of mode. The splitting failure of the concrete core as shown in Fig. 10(b) is characterized by the through vertical cracks that splitting the concrete block into two or more pieces. Most of the specimens (except T1, T5, T7~8) were observed to fail in this mode. The headed studs in specimen T5, T7, and T8 all failed in tensile fracture mode as shown in Fig. 10(c).

4.2 Effect of inclination angle θ

Fig. 11(a) shows the influence of the inclination angle θ on the tensile resistance of headed stud in DSC structure. It shows that the θ has more significant influence on the studs with height of 70 mm and 80 mm. For specimens with headed stud in height of 70 mm and 80 mm, their tensile resistances increase linearly with the increase of the θ. As the θ value increases from 30 to 60 degree, the tensile resistance of the headed stud in DSC specimen increases by about 20%. This is due to that as θ value increases, the average quantity of headed studs distributed on the tensile fracture cone increases the confinement on the fracture cone. However, for the headed stud with height of 90 mm, the increased height of the stud leads to the blowout failure of the connectors that compromises its tensile resistance.

(a) Breakout failure of the concrete core in specimen T1

(b) Splitting failure of concrete core in specimen T2

6

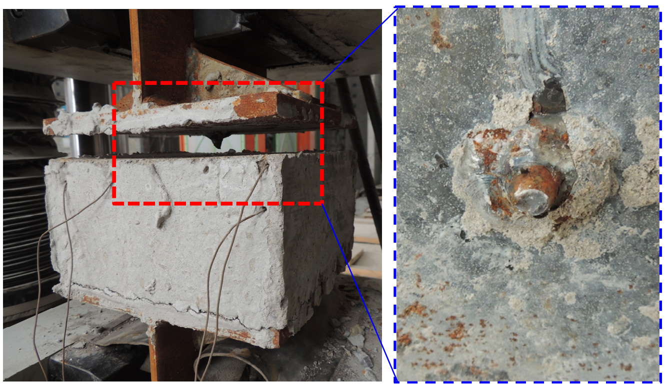

(c)Tensile fracture of specimen T8

Fig. 10 Different failure mode observed from the tension test on headed studs

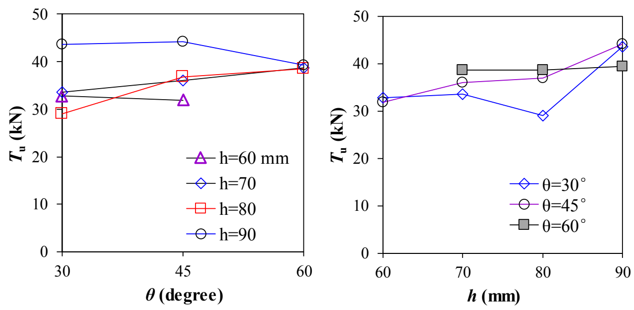

(a) Effect of θ (b) Effect of h

Fig. 11 Effect of θ and h on ultiamte tensile resistance of headed stud

4.3 Effect of height of the headed stud h

For the headed studs with θ value of 30 and 45 degrees, their tensile resistances increased almost linearly with the increase of their heights. As the height of the headed stud increases from 60 mm to 90 mm, its tensile resistance increases averagely by about 35%. This is because that, with the fixed depth of the concrete core and inclination angle θ, increasing the height of the headed stud resulted in higher projection area of the failure cone that finally resulted in higher tensile resistance of headed stud. However, for the headed studs with θ value of 60 degree, increasing the height of the headed stud exhibits ignorable influence on the tensile resistance of the headed stud. The explanation is that as the θ value equals 60 degree increasing the height of headed stud will not change the projection area of breakout cone in the concrete core since it is more influenced by the spacing of the connectors. Thus, the tensile resistance of the connectors exhibits less correlation with the height of the headed studs under this certain condition.

5. Analysis on shear and tensile resistance of the headed studs in DSC structure

5.1 Shear resistance of headed studs in DSC structure

The shear resistance of headed stud in DSC structure can be governed by the minor value of shank shear resistance of stud and concrete bearing capacity of the concrete. In Eurocode 4 (2004), the shear resistance of the headed stud can be determined as the following

$$P = \min\left(0.8 f_u \frac{\pi d^2}{4\gamma_v}, 0.29\alpha d^2 \sqrt{f_c E_c} / \gamma_v\right) \tag{1}$$

$$\alpha = \begin{cases} 0.2\left(h/d+1\right) & 3 \le h/d \le 4 \\ 1.0 & h/d \ge 1 \end{cases} \tag{2}$$

where d denotes diameter of the headed stud; f_u denotes ultimate strength of headed stud; f_c and E_c denote compressive strength and modulus of elasticity of concrete; h denotes height of headed stud; γ_v denotes partial safety factor, and equals to 1.25 (1.0 was used for the comparisons of the predictions with the test results).

In AASHTO/LRFD (2004), the shear resistance of the headed stud in steel-concrete composite structure can be determined by

$$P = 0.5\phi A_s \sqrt{f_c E_c} \le \phi f_u A_s \tag{3}$$

where, as denotes cross-sectional area of headed stud; f_c and E_c denote compressive strength and modulus of elasticity of the concrete, respectively; ϕ denotes resistance factor for headed stud and equals to 0.85.

5.2 Tensile resistance of the headed stud in DSC structure

Tensile resistance of a single headed stud may be governed by the minor value of the concrete breakout resistance (T_{CB}), pullout failure (T_{pl}), ultimate tensile resistance of the steel shank of the headed stud (T_s) , and punching shear resistance of the steel face plates (T_{ps}) (Yan *et al.* 2014a, 2015), i.e.

$$T = \min\begin{Bmatrix} T_{CB} = 0.33\sqrt{f_c} A_N / \gamma_c \\ T_{pl} = 8 A_{brg} f_{ck} / \gamma_c \\ T_s = A_s \sigma_u / \gamma_{M2} \\ T_{ps} = \pi d t \left(f_{ys} / \sqrt{3}\right) / \gamma_{M0} \end{Bmatrix} \tag{4}$$

where h_s is the connector's effective height; A_{brg} is the bearing area under tension for the headed stud; γ_{M2} is partial safety factor for steel under tension; γ_{M0} is partial factor for resistance of cross-section; A_N denotes the projection area of the breakout cone of concrete core.

For single headed stud, A_N can be calculated as the following

$$A_N = \pi\left(h_s + \frac{d_h}{2}\right)^2 - \frac{\pi}{4} d_h^2 \tag{5}$$

However, the dense layout of the headed studs in DSC shear wall structures may affect the mature development of the breakout cone in concrete core. Thus, the projection area needs to be modified as shown in Fig. 12.

Therefore, in DSC shear wall structure, the projection area (A_N) for the determination of the breakout resistance of the headed stud can be determined as the following

$$A_N = \begin{cases} (\pi - 2\phi + 2\sin\phi)\left(h_s + \frac{d_h}{2}\right)^2 - \frac{\pi}{4} d_h^2 & \sqrt{2}\left(h_s + d_h/2\right) \le S \le 2h_s + d_h \\ S^2 & S \ge 2h_s + d_h \end{cases} \tag{6}$$

where, ϕ denotes the angle as shown in Fig. 12, and ϕ = $\cos^{-1}[S/(2h_s + d_h)]$; S denotes the spacing of the headed stud in DSC shear wall; d_h denotes the diameter of the headed of the headed stud; h_s denotes the height of the shank of the headed stud.

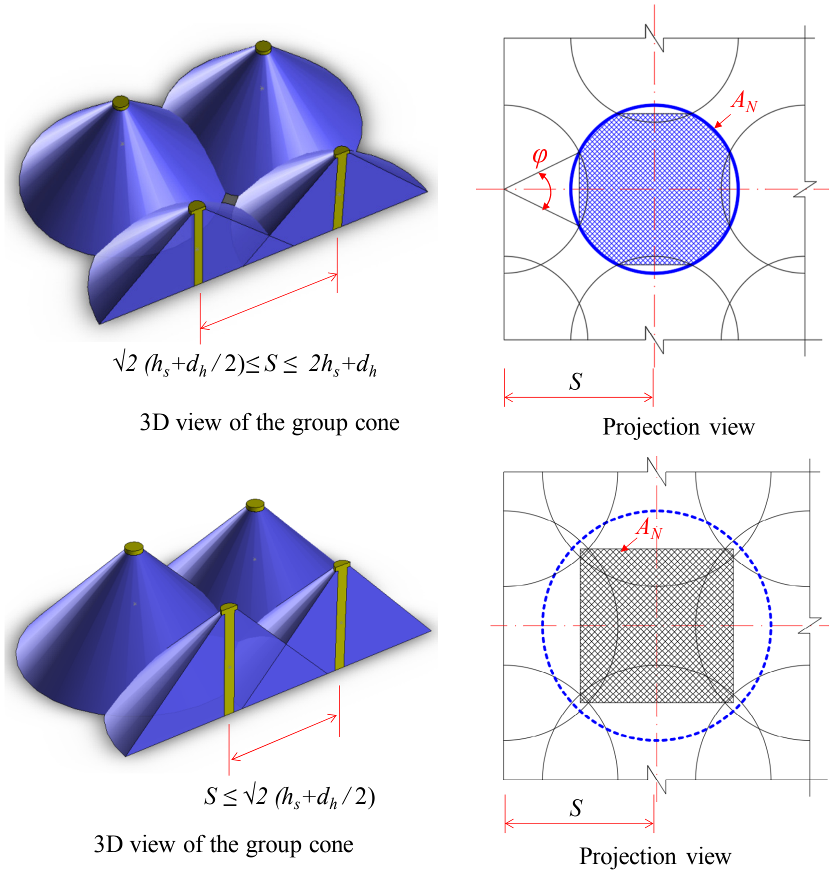

Fig. 12 Determination of the projection area A_N for the breakout failure of the headed stud in DSC shear wall

5.3 Validations

Before performing the validations, it should be noted that all the partial safety factors in Eqs. (1)~(6) were taken as 1.0. Tables 1 and 2 compares the predicted shear and tensile resistances of headed studs in the DSC shear wall with those predicted values by the developed analytical models in Eqs. (1)~(6). These tables show that both design equations in Eurocode 4 (2004) and AASHTO (2004) underestimates the shear resistance of headed shear studs in the DSC shear walls. The average test-to-prediction ratios for the Eurocode 4 (2004) equation (i.e., Eq. (1)) and AASHTO equation (i.e., Eq. (3)) are, respectively, 1.26 and 1.09 with the same Coefficient of Variation (COVs) of 0.14. The Eurocode 4 equation is more conservative on predicting the shear resistance of headed stud in DSC shear wall compared with the AASHTO (2004) equation. Thus, these two methods are recommended to predict the shear resistance of the headed stud in DSC shear wall.

Table 2 also shows that the developed analytical model, i.e., Eqs. (4)~(6) averagely underestimates the tensile resistance of the headed stud connectors in DSC shear wall by 7%. The COV for the 11 predictions is 0.19. The variations of the predictions maybe caused by the large scatter of the tensile strength of the concrete, the influence of the neighbouring headed studs attached to the opposite steel face plate, and dimension of the specimens. Thus, Eqs. (4)~(6) can be used to estimate the tensile resistance of headed stud connectors used in DSC shear wall structure.

6. Conclusions

This paper studied the shear and tensile behaviors of the headed stud connectors by full scaled tests and analytical methods. The structural behaviors of the headed stud under shear and tension were firstly studied through 22 tests. Analytical methods were developed to predict the ultimate shear and tensile resistances of the headed stud in DSC shear wall structure through modifying equations in design codes. Based on these experimental and analytical studies, the following conclusions can be drawn;

- Due to the weak confinement of the concrete core, most of the specimens failed in concrete splitting mode. The shear resistance of the headed studs in DSC shear wall was influenced by the height and layout of the connectors inside the structure, and these influences show high scatter in the shear resistance of the headed studs. The differences of the height and layout of the connectors in the specimens produced the differences in the confinement of the concrete that resulted in different shear resistances of the headed stud in the DSC shear wall.
- Increasing the value of θ (a geometric parameter as shown in Fig. 4) from 30 to 45 degree averagely increased the ultimate shear resistance of the headed stud by 20%. However, as θ increases from 45 to 60 degree its influence on the shear resistance of the headed stud becomes weak. Increasing the height of

headed stud from 60 mm to 90 mm slightly increases the shear resistance of headed stud.

- Tensile test results show that major failure mode of the headed stud under tension are splitting and breakout in concrete core, and tensile fracture of the steel shank. Increasing the θ value from 30 to 60 degree leads to 20% increment on tensile resistance of the headed stud with height of 70 mm and 80 mm. For specimens with θ value of 30 and 45 degrees Increasing the height of headed stud from 60 mm to 90 mm lead to an average increment of about 30% in the ultimate tensile resistance.
- Analytical models were developed to predict the shear and tensile resistances of the headed stud in DSC shear wall through modifying code equations. The dense layout of the connectors was also considered in the proposed analytical models. The validations of the predictions against 22 tests showed that the developed analytical models averagely underestimated the shear and tensile strength of the headed studs by 9% and 7%, respectively.

The above conclusions were based on limited experimental and analytical studies, and more tests were still required for further study on these related topics.

Acknowledgments

The authors would like to acknowledge the research grant 2016A06 received from the Scientific Research Fund of Institute of Engineering Mechanics, CEA, 2016YFC0701101 sponsored by the National Key Research and Development Program of China, and 51378478, 51608358, 51678538 received from National Natural Science Foundation of China for the works reported herein. The authors gratefully express their gratitude for the financial supports.

References

AASHTO (2004), LRFD bridge design specifications; 3rd Edition, Washington, D.C., USA.

ACI Committee 318 (2008), Building code requirements for structural concrete (ACI 318-08) and commentary (ACI 318R-08); American Concrete Institute, Farmington Hills, MI, USA.

ACI Committee 349 (2001), Code Requirements for Nuclear Safety Related Concrete Structures (ACI 349-01) and Commentary (ACI 349R-01); American Concrete Institute, Farmington Hills, MI, USA.

An, L. and Cederwall, K. (1996), "Push-out tests on studs in high strength and normal strength concrete", *J. Constr. Steel Res.*, **36**(1), 15-29.

ANSI/AISC. AISC 360-10 (2010), Specification for structural steel buildings; American National Standards Institute, Chicago, IL, USA.

CEB-FIP (1993), CEB-FIP model code 1990; Comité Euro-International Du Béton, Redwood Books, Trowbridge, Wiltshire, UK.

Cook, R.A., Collins, D.M., Klingner, R.E. and Polyzois, D. (1992), "Load-deflection behaviour of cast-in-place and retrofit concrete anchors", *ACI Struct. J.*, **89**(6), 639-649.

Eligehausen, R. and Balogh, T. (1995), "Behaviour of fasteners loaded in tension in cracked reinforced concrete", *ACI Struct. J.*, **92**(3), 365-379.

Eurocode 4 (2004), Design of composite steel and concrete structures-Part 1.1: General rules and rules for buildings, BS EN 1994-1-1:2004; Brussels, Belgium.

Fuchs, W., Eligehausen, R. and Breen, J.E. (1995), "Concrete capacity design (CCD) approach for fastening to concrete", *ACI Struct. J.*, **92**(1), 73-94.

Hamad, B.S., Haidar, Y.A. and Harajli, M.H. (2011), "Effect of steel fibers on bond strength of hooked bars in normal-strength concrete", *ACI Struct. J.*, **108**(1), 42-50.

Han, Q.H., Xu, J., Xing, Y. and Li, Z.L. (2015), "Static push-out test on steel and recycled tire rubber-filled concrete composite beams", *Steel Compos. Struct., Int. J.*, **19**(4), 843-860.

Han, Q.H., Wang, Y.H. and Xu, J. (2017), "Numerical analysis on shear stud in push-out test with crumb rubber concrete", *J. Constr. Steel Res*, **130**, 148-158.

Hu, H.S., Nie, J.G. and Eatherton, M.R. (2014), "Deformation capacity of concrete-filled steel plate composite shear walls", *J. Constr. Steel Res.*, **103**, 148-158.

Ji, X., Sun, Y., Qian, J. and Lu, X. (2015), "Seismic behaviour and modeling of steel reinforced concrete (SRC) walls", *Earthq. Eng. Struct. Dyn.*, **44**(6), 955-972.

Ji, X., Cheng, X., Jia, X. and Varma, A.H. (2017), "Cyclic in-plane shear behaviour of double skin composite shear walls in high-rise buildings", *J. Struct. Eng. ASCE*, **143**(6), 04017025.

Kurt, E.G., Varma, A.H., Booth, P. and Whittaker, A.S. (2016), "In-plane behaviour and design of rectangular SC wall piers without boundary elements", *J. Struct. Eng. ASCE*, **142**(6), 04016026.

Leekitwattana, M., Boyd, S.W. and Shenoi, R.A. (2011), "Evaluation of the transverse shear stiffness of a steel bi-directional corrugated-strip-core sandwich beam", *J. Constr. Steel Res.*, **67**(2), 248-254.

Lynch, T.J. and Burdette, E.G. (1991), "Some design considerations for anchors in concrete", *ACI Struct. J.*, **88**(1), 91-97.

Malek, N., Machida, A., Mutsuyoshi, H. and Makabe, T. (1993), "Steel-concrete sandwich members without shear reinforcement", *Transact. Japan Concrete Inst.*, **15**(2), 1279-1284.

Narayanan, R., Bowerman, H.G., Naji, F.J., Roberts, T.M. and Helou, A.J. (1997), "Application guidelines for Steel-Concrete-Steel sandwich construction-1: Immerses Tube Tunnels", SCI publication 132, The Steel Construction Institute, Ascot, Berkshire, UK.

Nie, J.G., Hu, H.S., Fan, J.S., Tao, M.X., Li, S.Y. and Liu, F.J. (2013), "Experimental study on seismic behavior of high-strength concrete filled double-steel-plate composite wall", *J. Constr. Steel Res.*, **88**, 206-219.

Oehlers, D.J. and Johnson, R.P. (1987), "The strength of stud shear connections in composite beams", *Struct. Engr.*, **65**B(2), 44-48.

Ollgaard, J.G., Slutter, R.G. and Fisher, J.W. (1971), "Shear strength of stud connectors in lightweight and normal-weight concrete", *AISC Eng. J.*, **8**(2), 55-64.

Roberts, T.M. and Dogan, O. (1998), "Fatigue of welded stud shear connectors in steelconcrete-steel sandwich beams", *J. Constr. Steel Res.*, **45**(3), 301-320.

Sener, K. and Varma, A.H. (2014), "Steel-plate composite SC walls: Experimental database and design for out-of-plane shear", *J. Constr. Steel Res.*, **100**, 197-210.

Shanmugam, N.E., Kumar, G. and Thevendran, V. (2002), "Finite element modelling of double skin composite slabs", *Finite Elem. Anal. Des.*, **38**(7), 579-599.

Slobodan, R. and Dragoljub, D. (2002), "Static strength of the shear conectors in steel-concrete composite beams-regulations and research analysis", *Architect. Civil Eng.*, **2**(4), 251-259.

Tomlinson, M., Chapman, M., Wright, H.D., Tomlinson, A. and Jefferson, A.D. (1990), “Shell Composite Construction for Shallow Draft Immersed Tube Tunnels”, *Proceedings of the ICE International Conference on Immersed Tube Tunnel Techniques*, Manchester, Thomas Telford, London, UK, pp. 209-220.

Viest, I.M. (1957), “Investigation of Stud Shear Connectors for Composite Concrete and Steel T-Beams”, *J. Am. Concrete Inst.*, **52**(4), 875-892.

Wright, H.D., Oduyemi, T.O.S. and Evans, H.R. (1991), “The experimental behaviour of double skin composite elements”, *J. Constr. Steel Res.*, **19**(2), 97-110.

Xie, M. and Chapman, J.C. (2005), “Static and fatigue tensile strength of friction-welded bar–plate connections embedded in concrete”, *J. Constr. Steel Res.*, **61**(5), 651-673.

Xue, W.C., Ding, M., Wang, H. and Luo, Z.W. (2008), “Static behaviour and theoretical model of stud shear connectors”, *J. Bridge Eng.*, **13**(6), 623-634.

Yan, J.B., Liew, J.Y.R. and Zhang, M.H. (2014a), “Tensile resistance of J-hook connectors in steel-concrete-steel sandwich composite structure”, *J. Constr. Steel Res.*, **100**, 146-162.

Yan, J.B., Liew, J.Y.R., Zhang, M.H. and Wang, J.Y. (2014b), “Ultimate strength behaviour of steel-concrete-steel sandwich composite structures, Part 1: Experimental and analytical Study”, *Steel Compos. Struct., Int. J.*, **17**(6), 907-927.

Yan, J.B., Liew, J.Y.R. and Zhang, M.H. (2015), “Shear-tension interaction strength of J-hook connectors in steel-concrete-steel sandwich structure”, *Adv. Steel Constr.*, **11**(1), 72-93.

Yan, J.B., Liu, X.M., Liew, J.Y.R., Qian, X. and Zhang, M.H. (2016), “Steel-concrete-steel sandwich system in Arctic offshore structures: Materials, experiments, and design”, *Mater. Des.*, **91**, 111-121.

Zamora, N.A., Cook, R.A., Konz, R.C. and Consolazio, G.R. (2003), “Behaviour and design of single, headed and unheaded, grouted anchors under tensile load”, *ACI Struct. J.*, **100**(2), 222-230.

Zhang, K., Varma, A.H., Malushte, S. and Gallocher, S. (2014), “Effects of shear connectors on the local buckling and composite action in steel concrete composite walls”, *Nucl. Eng. Des.*, **269**, 231-239.

DL